

## Simulation of formation and evolution of nano-clusters during rapid solidification of liquid $\text{Ca}_{70}\text{Mg}_{30}$ alloy

Li-li ZHOU<sup>1,2</sup>, Rang-su LIU<sup>2</sup>, Ze-an TIAN<sup>2,3</sup>

1. Department of Information Engineering, Gannan Medical University, Ganzhou 341000, China;

2. School of Physics and Microelectronics Science, Hunan University, Changsha 410082, China;

3. School of Materials Science and Engineering, University of New South Wales, Sydney NSW 2052, Australia

Received 17 July 2012; accepted 27 November 2012

**Abstract:** A molecular dynamics simulation study was performed to investigate the formation and evolution mechanisms of nano-clusters during the rapid solidification of liquid  $\text{Ca}_{70}\text{Mg}_{30}$  alloy. The cluster-type index method (CTIM) was adopted to describe microstructure evolutions of nano-clusters during solidification. Results indicate that amorphous structure is mainly formed with three bond-types of 1551, 1541 and 1431 at the cooling rate of  $5 \times 10^{11}$  K/s, and glass transition temperature  $T_g$  is about 530 K; the icosahedron cluster of (12 0 12 0) plays a key role in formation of amorphous structure, and smaller Mg atoms are much more probable to be central atoms of icosahedron clusters; and nano-clusters are mainly formed by combining medium-size clusters. Interestingly, it was also found that formation and evolution processes of the nano-cluster display a three-stage feature which is analogous to crystallization process of amorphous alloy.

**Key words:** nano-clusters;  $\text{Ca}_{70}\text{Mg}_{30}$  alloy; rapid solidification; molecular dynamics simulation

### 1 Introduction

It is well known that the Ca–Mg and Ca–Mg based alloys are extremely promising materials for applications in industry, due to their virtues of high intensity, low density, easy for jointing and so on. Moreover, they are also considered potential candidates for applications as a new kind of implant biomaterials because of their suitable mechanical properties, inherent biocompatibilities and biodegradabilities [1–3]. These intriguing advantages have inspired widespread attention on the investigation of Ca–Mg and Ca–Mg based alloys [1–8]. For example, LI et al [2] studied the influence of Ca content on the property of binary Mg–Ca alloy as biomedical implant material; molecular dynamics simulations of 500 particles were performed by QI and WANG [4] to study the icosahedral order and the defects in the supercooled and amorphous  $\text{Ca}_7\text{Mg}_3$  alloy; HOU et al [5] detected the short-range and medium-range

orders in the metallic  $\text{Ca}_7\text{Mg}_3$  alloy. These results are complementary to each other that provide deep understanding of structures and properties for Ca–Mg alloys.

Macroscopical performance of a material is largely determined by its microstructure of nano-clusters formed during the solidification. The nano-clusters that are the congeries of several or thousands of atoms, are bridge of microstructures and macro-bulks of materials. Therefore, the comprehension of growth mechanism of nano-clusters is very important. However, the investigation of formation and evolution processes of nano-clusters at atomic level is still very difficult in experiment, due to small size and very short time scale. Fortunately, molecular dynamics simulation is an effective remedy.

In this work, a molecular dynamics simulation is performed to study the formation and evolution of clusters, especially of those containing hundreds or thousands of atoms, which form in the supercooled liquid and metallic glass of  $\text{Ca}_{70}\text{Mg}_{30}$  alloy.

**Foundation item:** Project (50831003) supported by the National Natural Science Foundation of China; Project (20114BAB215026) supported by Jiangxi Provincial Natural Science Foundation, China; Project (ZD201002) supported by Fund for Basic Scientific Research of Gannan Medical University, China

**Corresponding author:** Li-li ZHOU; E-mail: [lilizhou369@gmail.com](mailto:lilizhou369@gmail.com)

DOI: 10.1016/S1003-6326(13)62741-7

## 2 Simulation

The interaction among atoms of Ca–Mg alloy was calculated via effective pair potential function of generalized nonlocal model-pseudopotential (GNMP) which was developed by WANG et al [9,10]. And the function is given by

$$V(r) = (Z_{\text{eff}}^2 / r) \left[ 1 - \left( \frac{2}{\pi} \right) \int_0^\infty dq F(q) \sin(rq) / q \right] \quad (1)$$

where  $Z_{\text{eff}}$  is the effective ionic valence, and  $F(q)$  is the normalized energy wave number characteristic, and both were defined in Refs. [9,10]. The reliability of the potential for Ca–Mg alloy has been demonstrated by computing its structure characteristics [4,5]. The pair potential is cut off at 20 a.u. (atom unit).

The MD simulation was carried out in a cubic box with 10000 atoms (7000 Ca atoms and 3000 Mg atoms) under ambient pressure [11] and subjected to periodic boundary conditions. The motion equations were integrated using the leapfrog algorithm with the time step of 5 fs. The rapid solidification process was started at 1173 K; first of all, system ran 50000 time steps to obtain equilibrium liquid state determined by energy change of the system; in cooling process, temperature of the system was decreased to 323 K with a cooling rate of  $5 \times 10^{11}$  K/s. The interval between two temperature points was 50 K. In this work, the system temperature was controlled by damped force method [12,13]. At each selected temperature, microstructure was quantified by HA bond-type index method [14], cluster type index method (CTIM) [15–17], and extended cluster analysis method [17, 18] based on the CTIM.

## 3 Results and discussion

### 3.1 $S(Q)$ and $g(r)$ analysis

First of all, the total pair distribution function of  $g(r)$  is calculated from the  $\text{Ca}_{70}\text{Mg}_{30}$  system at 323 K, and transformed to  $S(Q)$  through the Fourier transformation, and compared with the experimental result at the same temperature given by NASSIF et al [19], as shown in Fig. 1. Figure 1 shows that simulation result is well agreed with experimental result both in the position of peaks and splitting spot of second peak; except for slight lower height of the first peak. The disagreement can be comprehended by realizing that much higher cooling rate adopted in the present simulation than that in experiment will lead to a lower degree of short-range order resulting in lower height of the first peak of  $S(Q)$  evidently [20]. Thus, this indicates that the effective pair-potential adopted here is successful in reflecting the objective physical nature of this system.

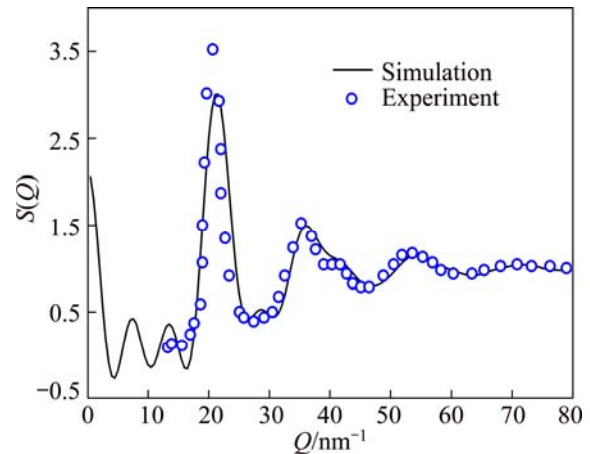


**Fig. 1** Comparison of  $S(Q)$  for  $\text{Ca}_{70}\text{Mg}_{30}$  metallic glass at 323 K between simulation and experimental results [8,19]

The Wendt-Abraham parameter [21] is adopted to determine glass transition temperature  $T_g$  of  $\text{Ca}_{70}\text{Mg}_{30}$  system during rapid solidification. It is defined as

$$R = g(r)_{\text{min}} / g(r)_{\text{max}} \quad (2)$$

where  $g(r)_{\text{min}}$  and  $g(r)_{\text{max}}$  are magnitudes of the first shell maximum and the first minimum following this maximum in pair distribution functions, respectively. And  $T_g$  is turning point of the curve slope. Figure 2 shows that intersection of two straight lines indicates glass transition being at about 530 K. It is lower than the result of HOU et al [5] obtained at a higher cooling rate of  $1 \times 10^{12}$  K/s. Usually  $T_g$  decreases with decreasing cooling rate [20,22]. Thus, the result is also logical compared with simulation result of BARNETT et al [6], they simulated the rapid solidification process of  $\text{Ca}_{67}\text{Mg}_{33}$  alloy (the composition is close to  $\text{Ca}_{70}\text{Mg}_{30}$ , and the result is comparable in some extent) with a cooling rate of  $3.2 \times 10^{13}$  K/s, and obtained  $T_g = 570$  K.

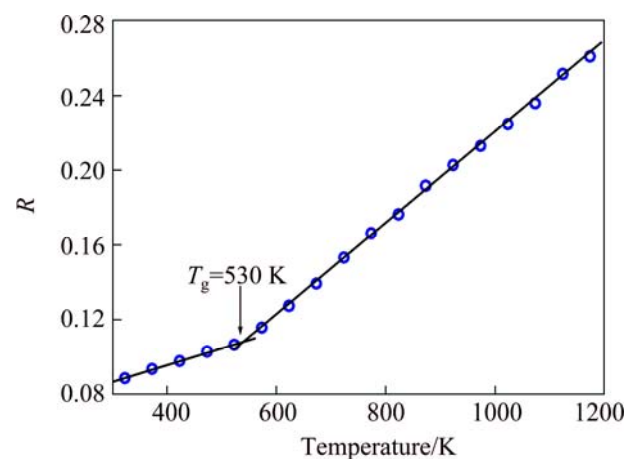


**Fig. 2** Temperature dependence of Wendt-Abraham parameter  $R$  during rapid solidification

### 3.2 HA bond-type index

HA bond-type index method, proposed by HONEYCUTT and ANDERSEN [14], can be used to well describe and discern the concrete relationship of an atom with its near neighbors. For a long time, HA bond-type index method has been widely and successfully used to describe and analyze microstructural evolutions during phase transitions [15–18]. When local configurations are described by HA bond-type index method, the 1551, 1541 and 1431 bond-types are characteristic bond-types of typical liquid and amorphous states [15–18].

Figure 3 shows evolutions of relative numbers of various bond-types during cooling process of  $\text{Ca}_{70}\text{Mg}_{30}$  alloy. It shows that most of the bond-types change slightly, only the 1551 bond-type increases distinctly with the decreasing temperature. This indicates that amorphous structure is freeze of liquid structure in some extent, in other words, many local configurations characterized by various HA bond-type indices in metallic glass are inherited from liquid. The total relative number of bond-types of 1551, 1541 and 1431 is 50.95% at 1173 K, and increases to 75.96% at 323 K. This means that the 1551, 1541 and 1431 bond-types play a key role in the glass transition process.

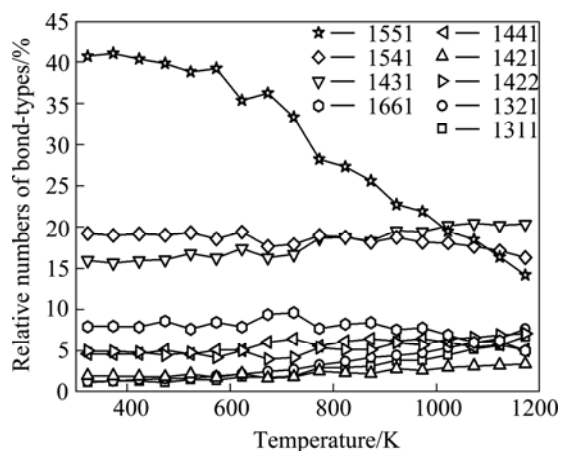


Fig. 3 Relative numbers of bond-types as function of temperature

### 3.3 Icosahedron cluster analysis

However, HA bond-type index method is incapable of describing cluster composed of more than ten atoms, especially the nano-clusters. So, the cluster type index method (CTIM) [16–18] is adopted to describe microstructural evolutions of the system. In CTIM, a basic cluster is defined as structure composed of a core atom and its surrounding neighbor atoms. A set of four integers are adopted to describe a basic cluster. The first integer represents total number of near-neighbors of center atom, and following three integers equal to the numbers of 1441, 1551, and 1661 bond-types,

respectively, by which surrounding atoms are connected with center atom. With CTIM, basic cluster of an icosahedron can be identified as (12 0 12 0). Figure 4 shows that there are three typical basic clusters in the present simulation system.

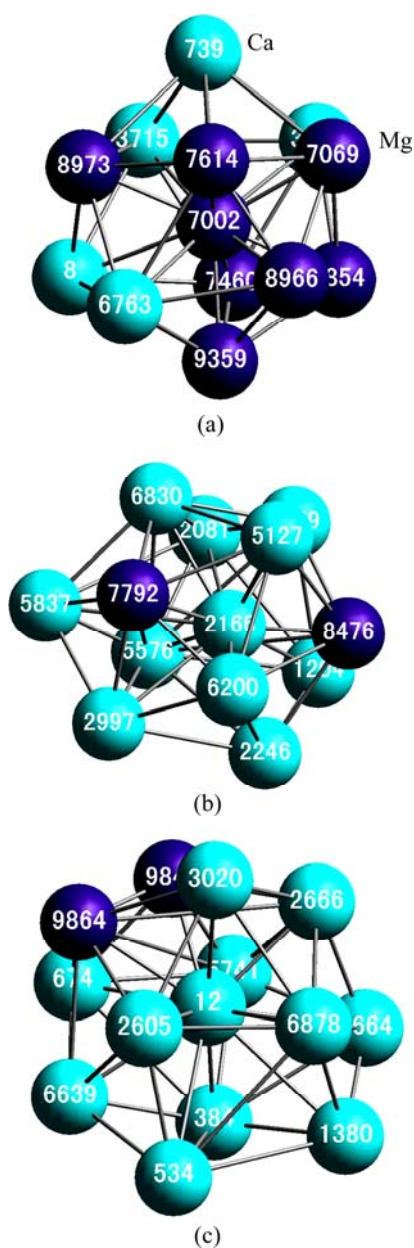


Fig. 4 Schematics for three typical basic clusters in  $\text{Ca}_{70}\text{Mg}_{30}$  system (light blue is for Ca atoms, and dark purple is for Mg atoms): (a) (12 0 12 0); (b) (12 2 8 2); (c) (13 1 10 2)

According to CTIM, numbers of various basic clusters in  $\text{Ca}_{70}\text{Mg}_{30}$  system at given temperatures can be obtained, as shown in Fig. 5. All types of basic clusters remain few until at the temperature of 873 K and then they increase as temperature decreases. Among them, the basic clusters of (12 0 12 0) increases remarkably, especially in the temperature range of  $523 \text{ K} < T < 873 \text{ K}$ , and it almost keeps constant when the temperature is

below 523 K. It further confirms that glass transition occurs at around 523 K, which is consistent with above analysis for Wendt-Abraham parameter  $R$ . Besides the icosahedron basic cluster, defect icosahedral basic clusters of (12 2 8 2) and (13 1 10 2) (schematics for them are shown in Fig. 4 (b) and (c), respectively) also increase a little. Therefore, icosahedron basic cluster plays a key role in the formation of metallic glass of  $\text{Ca}_{70}\text{Mg}_{30}$ .

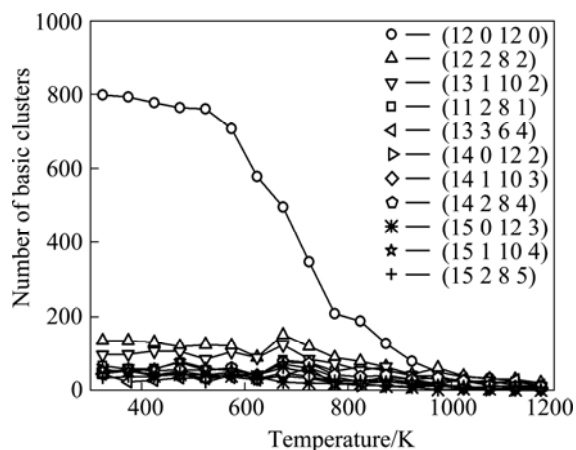


Fig. 5 Number of basic clusters as function of temperature

Figure 6 shows distributions of icosahedron basic clusters and their central atoms at three temperatures. It shows that these icosahedron basic clusters embedded in

the liquid structure isolated from each other at high temperature (Fig. 6(a)). With the decrease of temperature, the number of icosahedron basic clusters increases, and they are connected by intercross-sharing atoms in the form of chains or dendrites, as shown in Figs. 6(b) and (c). As temperature decreases to 323 K, the icosahedron basic clusters are amalgamated with each other in the system. The number of atoms in these icosahedron basic clusters reaches 7969 (79.69 %). It further confirms that icosahedron structure plays a leading role in the formation of metallic glass of  $\text{Ca}_{70}\text{Mg}_{30}$  alloy.

Figure 6 shows that most of icosahedrons are Mg-centered (dark purple). Going further, the numbers of icosahedron basic clusters are calculated with central atom of Ca and Mg at different temperatures, respectively, as shown in Fig. 7. Obviously, overwhelming number of icosahedron basic clusters are with Mg as central atom at all temperatures concerned. That is to say, the smaller atom is much more probable to be the central atom of icosahedron basic cluster. It can be interpreted from the view point of geometry that configuration with smaller atom as centre will be more compact, and the configuration will be much more stable. This is coincide with the result of YANG and ZHAO [23], where they argued that central sites of icosahedrons prefer to choose smaller atoms, while neighbor sites do not have any bias.

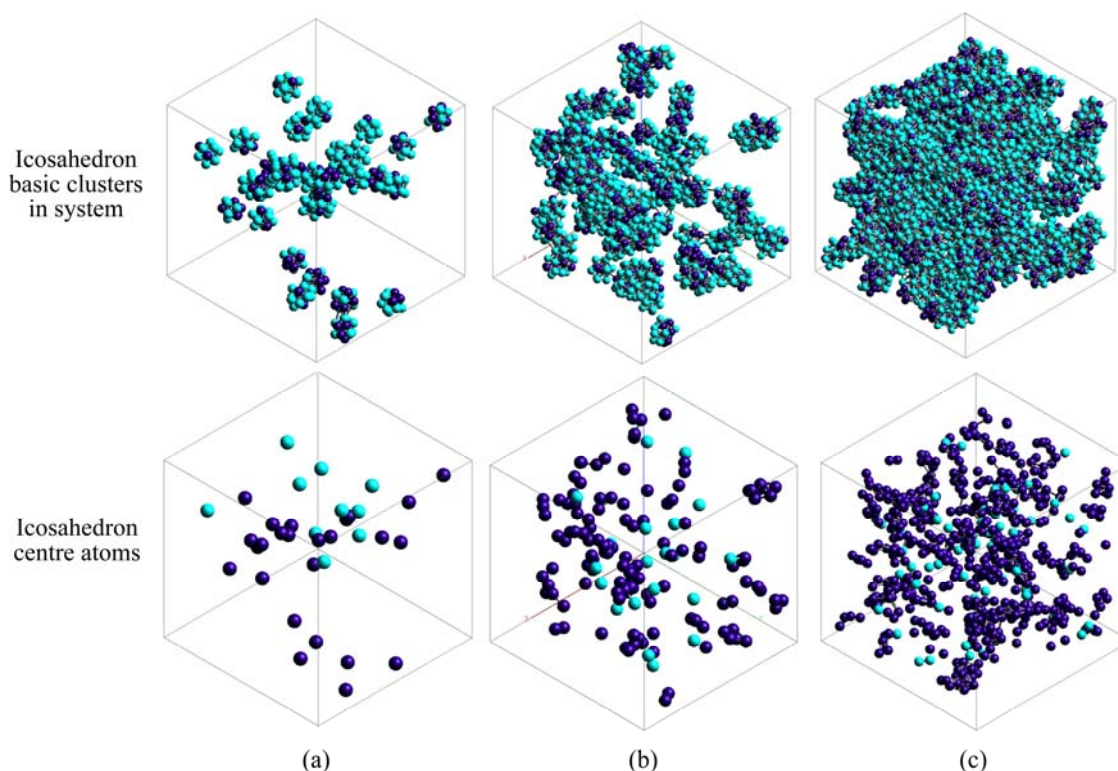
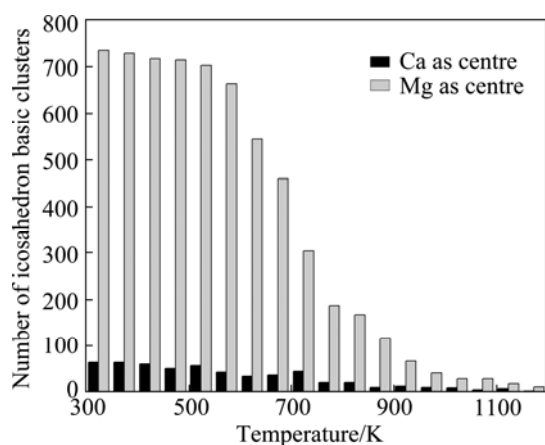


Fig. 6 3D snapshots for icosahedron basic clusters and their central atoms in the system at three temperatures (Light blue is for Ca atoms, and dark purple is for Mg atoms): (a) 973 K; (b) 773 K; (c) 323 K



**Fig. 7** Histogram for numbers of icosahedron basic clusters with central atom of Ca and Mg at temperatures concerned, respectively

### 3.4 Formation and evolution characteristic of nano-clusters

When different basic clusters are connected with each other as their centre bonded, some larger clusters of different size can be formed. Thus, atoms in the larger clusters are more tightly connected to each other, and the cluster would be more stable.

Figure 8 shows temperature dependence of total number of basic clusters, total number of clusters, and size of maximum cluster in the system, respectively. According to Fig. 8, the formation and evolution of clusters of  $\text{Ca}_{70}\text{Mg}_{30}$  during the rapid solidification process can be divided into three stages. In stage I (1173–873 K), the total number of basic cluster is 166 at 1173 K, and increased to 674 at 873 K; meanwhile, the total number of clusters is 83 at 1173 K, and increased to 205 at 873 K; while the size of maximum cluster remains small. This indicates that many small clusters are formed and embedded in the liquid structure isolated, and these small clusters can be formed and disappeared randomly due to the structural fluctuation of supercooled liquid. In stage II (873–530 K), the total number of basic cluster still increases, while the total number of cluster decreases, and meanwhile, the size of the maximum cluster increases sluggishly. This indicates that small basic clusters begin to merge with surrounding ones, and medium-size clusters are formed. In stage III (530–323 K), both the total numbers of basic clusters and clusters are almost constant; while the size of the maximum cluster increases abruptly; this phenomenon can be interpreted as follow. As in glass state at this temperature range, the atoms are almost being “frozen”; however, the local clusters can still collectively move with structure fluctuation, and the system evolves toward configuration with lower energy; thus, the medium-size cluster can be

further combined with each other, and a nano-cluster contained 2374 atoms is finally formed in the system at 323 K.

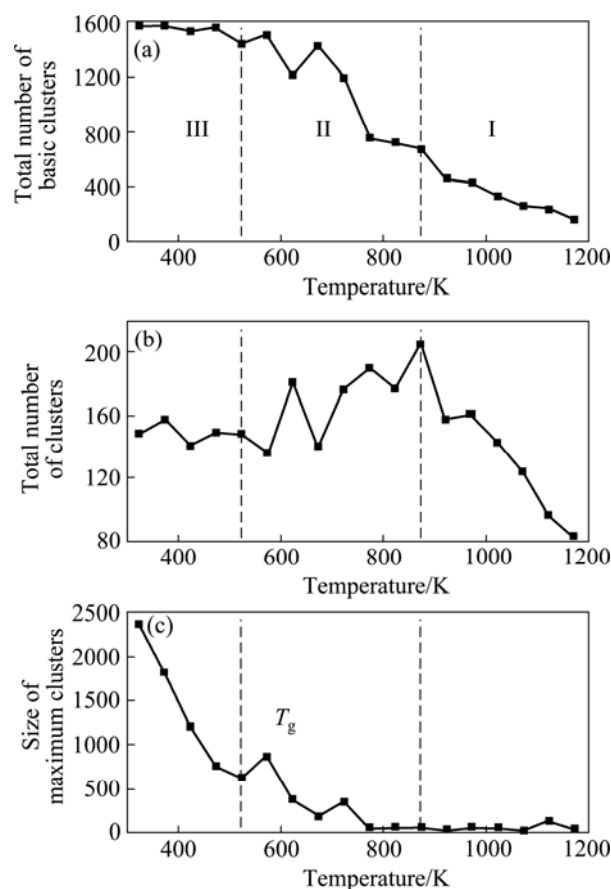


**Fig. 8** Total number of all basic clusters (a), clusters (b), and size of maximum cluster (c) as a function of temperature

It is worth pointing out that, in some respects, the three-stage feature in formation and evolution process of nano-cluster is analogous to crystallization process of amorphous alloys, which consist of crystal nucleation, grain growth and grain coarsening [24, 25]; that is, during the first stage, some small crystal nuclei occurs in the amorphous matrix; in the second stage, the sizes of nuclei obviously increase by consuming the surrounding amorphous phase; in the third stage, the crystal grains coarsening by merging other medium-size crystal grains. They are respectively corresponding to the three-stage feature of evolution process of nano-cluster: formation of instable small clusters at high temperature, small clusters grow into medium-size clusters, and nano-clusters are formed by combining multi medium-size clusters.

The snapshot for nano-cluster of 2374 atoms is shown in Fig. 9 (a), which consists of 24 types of 537 basic clusters 270 (12 0 12 0), 19 (14 0 12 2), 28 (15 0 12 3), 6 (16 0 12 4), 29 (13 1 10 2), 23 (14 1 10 3), 21 (15 1 10 4), 10 (16 1 10 5), 2 (10 2 8 0), 22 (11 2 8 1), 37 (12 2

8 2), 1 (13 2 8 3), 16 (14 2 8 4), 17 (15 2 8 5), 6 (16 2 8 6), 4 (12 3 6 3), 15 (13 3 6 4), 1 (14 3 6 5), 2 (15 3 6 6), 2 (17 3 6 8), 2 (11 4 4 3), 2 (12 4 4 4), 1 (15 4 4 7), and 1 (1 4 6 0 8). As it can be seen from Fig. 9, shape of nano-cluster is irregular, and there are some corners, which are suitable to be new starting points of dendrite growth in the system during rapid solidification. The shape of this nano-cluster is obviously different from those obtained by gaseous deposition, ionic spray methods and so on, since those nano-clusters are crystals or near crystals consisted of icosahedron shell structure with a central atom [26].

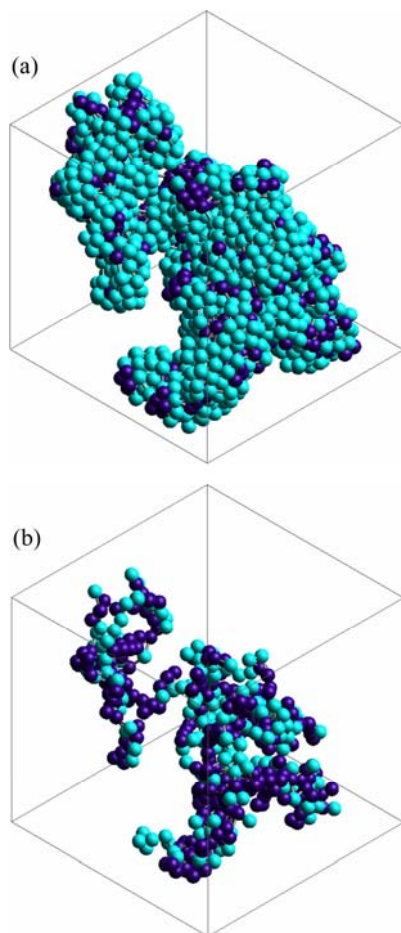


**Fig. 9** Snapshot of a nano-cluster formed at 323 K in system: (a) All atoms; (b) Only central atoms of maximum nano-cluster (light blue is for Ca atoms, and dark purple is for Mg atoms)

As mentioned above, formation and evolution process of nano-cluster has been exactly and clearly characterized by CTIM, which suggests that CTIM is an effective method for describing the disorder system of metallic glasses.

#### 4 Conclusions

1) Amorphous structure of  $\text{Ca}_{70}\text{Mg}_{30}$  alloy is formed mainly with 1551, 1541 and 1431 bond-types at cooling

rate of  $5 \times 10^{11}$  K/s, and glass transition temperature is about 530 K.

2) The icosahedron basic cluster of (12 0 12 0) plays a key role in the formation of amorphous structure, and the smaller Mg atoms are much more probable to be the central atoms of basic clusters of (12 0 12 0).

3) Formation and evolution process of nano-clusters in the system can be clearly and exactly described by CTIM, and result indicates that it exhibits three-stage feature: formation of instable small clusters at high temperature, small clusters grow into medium-size clusters, and formations of nano-clusters by combining of medium-size clusters. And it is analogous to crystallization process of amorphous alloys in some respects.

#### References

- [1] KIRKLAND N T, LESPAGNOL J, BIRBILIS N, STAIGER M P. A survey of bio-corrosion rates of magnesium alloys [J]. *Corrosion Science*, 2010, 52(2): 287–291.
- [2] LI Zi-jian, GU Xu-nan, LOU Si-quan, ZHENG Yu-feng. The development of binary Mg–Ca alloys for use as biodegradable materials within bone [J]. *Biomaterial*, 2008, 29(10): 1329–1344.
- [3] ZHANG Er-lin, YANG Lei. Microstructure, mechanical properties and bio-corrosion properties of Mg–Zn–Mn–Ca alloy for biomedical application [J]. *Mater Sci Eng A*, 2008, 497(1–2): 111–118.
- [4] QI D W, WANG S. Icosahedral order and defects in metallic liquids and glasses [J]. *Phys Rev B*, 1991, 44(2): 884–887.
- [5] HOU Zhao-yang, LIU Li-xia, LIU Rang-su, TIAN Ze-an, WANG Jin-guo. Short-range and medium-range order in  $\text{Ca}_{70}\text{Mg}_{30}$  metallic glass [J]. *J Appl Phys*, 2010, 107(8): 083511–083517.
- [6] BARNETT R N, CLEVELAND C L, LANDMAN UZI. Structure and dynamics of a metallic glass: Molecular-dynamics simulations [J]. *Phys Rev Lett*, 1985, 55(19): 2035–2038.
- [7] SUCK J B, RUDINT H, GUNTHERODT H J, BECK H. Dynamical structure factor of the metallic glass  $\text{Ca}_{70}\text{Mg}_{30}$  at room temperature [J]. *J Phys F: Met Phys*, 1981, 11(7): 1375–1383.
- [8] JASWAL S S, HAFNER J. Atomic and electronic structure of crystalline and amorphous alloys. I. Calcium-magnesium compounds [J]. *Phys Rev B*, 1988, 38(11): 7311–7319.
- [9] WANG S, LAI S K. Structure and electrical resistivities of liquid binary alloys [J]. *J Phys F: Metal Phys*, 1980, 10(12): 2717–2737.
- [10] LI D H, LI X R, WANG S. Variational calculation of Helmholtz free energies with applications to the sp-type liquid metals [J]. *J Phys F: Metal Phys*, 1986, 16(3): 309–321.
- [11] QI D W, MOORE R A. Molecular dynamics simulations for crystallization of metallic liquids under different pressures [J]. *J Chem Phys*, 1993, 99(11): 8948–8952.
- [12] HOOVER WILLIAM G, LADD ANTHONY J C, MORAN BILL. High-strain-rate plastic flow studied via nonequilibrium molecular dynamics [J]. *Phys Rev Lett*, 1982, 48(26): 1818–1820.
- [13] EVANS D J. Computer “experiment” for nonlinear thermodynamics of couette flow [J]. *J Chem Phys*, 1983, 78(6): 3297–3302.
- [14] HONEYCUTT J D, ANDERSON H C. Molecular-dynamics study of melting and freezing of small Lennard-Jones clusters [J]. *J Phys Chem*, 1987, 91(19): 4950–4963.
- [15] LIU Rang-su, DONG Ke-jun, TIAN Ze-an, LIU Hai-rong, PENG Ping, YU Ai-bing. Formation and magic number characteristics of clusters formed during solidification processes [J]. *J Phys: Condens Matter*, 2007, 19: 196103–196117.

- [16] ZHOU Li-li, LIU Rang-su, TIAN Ze-an, LIU Hai-rong, HOU Zhao-yang, ZHU Xuan-min, LIU Quan-hui. Formation and evolution characteristics of bcc phase during isothermal relaxation processes of supercooled liquid and amorphous metal Pb [J]. Transactions of Nonferrous Metals Society of China, 2011, 21(3): 588–597.
- [17] YI Xue-hua, LIU Rang-su, TIAN Ze-an, HOU Zhao-yang, LI Xiao-yang, ZHOU Qun-yi. Formation and evolution properties of clusters in liquid metal copper during rapid cooling processes [J]. Transactions of Nonferrous Metals Society of China, 2008, 18(1): 33–39.
- [18] LIU Rang-su, DONG Ke-jun, LI Ji-yong, YU Ai-bing, ZOU Ri-ping. Formation and description of nano-clusters formed during rapid solidification processes in liquid metals [J]. J Non-Cryst Solids, 2005, 351(6–7): 612–617.
- [19] NASSIF E, LAMPARTER P, STEEV S. X-ran diffraction study on the structure of the metallic glass  $Mg_{84}Ni_{16}$  and  $Mg_{30}Ca_{70}$  [J]. Z Naturforsch, 1983, 38a: 1206–1210.
- [20] VOLLMAYR K, KOB W, BINDER K. Cooling-rate effects in amorphous silica: A computer-simulation study [J]. Phys Rev B, 1996, 54(22): 15808–15827.
- [21] WENDT H R, ABRAHAM FARID F. Empirical criterion for the glass transition region based on monte carlo simulations [J]. Phys Rev Lett, 1978, 41(18): 1244–1246.
- [22] VOLLMAYR K, KOB W, BINDER K. How do the properties of a glass depend on the cooling rate? A computer simulation study of a Lennard-Jones system [J]. J Chem Phys, 1996, 105(11): 4714–4728.
- [23] YANG Quan-wen, ZHANG Tao. Molecular dynamics study of icosahedral clusters in Ni–Zr amorphous alloys [J]. Chin Phys Lett, 2006, 23(4): 915–918.
- [24] PEI Q X, LU C, LEE H P. Crystallization of amorphous alloy during isothermal annealing: A molecular dynamics study [J]. J Phys: Condens Matter, 2005, 17(10): 1493–1504.
- [25] LU K, ZHANG X H. Identification of crystal nucleation and growth in an amorphous FeZr<sub>2</sub> alloy by means of electrical resistance measurements [J]. Phil Mag Lett, 2000, 80(12): 797–805.
- [26] MARTIN T P. Shells of atoms [J]. Phys Report, 1996, 273(4): 199–241.

## 液态 $Ca_{70}Mg_{30}$ 合金快速凝固过程中 纳米团簇结构形成演变特性模拟

周丽丽<sup>1,2</sup>, 刘让苏<sup>2</sup>, 田泽安<sup>2,3</sup>

1. 赣南医学院 信息工程学院, 赣州 341000;

2. 湖南大学 物理与微电子科学学院, 长沙 410082;

3. School of Materials Science and Engineering, University of New South Wales, Sydney NSW 2052, Australia

**摘要:** 采用分子动力学方法对液态  $Ca_{70}Mg_{30}$  合金快速凝固过程中纳米团簇结构的形成和演变特性进行模拟。采用原子团类型指数法(CTIM)对凝固过程中纳米团簇结构的演变进行分析。结果表明: 系统在  $5 \times 10^{11}$  K/s 的冷速条件下形成以 1551、1541 和 1431 为主的非晶态结构, 非晶转变温度约为 530 K; (12 0 12 0)二十面体基本原子团对系统非晶结构的形成起到决定性的作用, 并且原子半径较小的 Mg 原子更容易占据二十面体基本原子团中心原子的位置; 同时, 纳米团簇主要是通过中等尺寸团簇的合并而形成, 纳米级大团簇的形成演变过程呈现出类似于非晶晶化过程的 3 个阶段式的变化。

**关键词:** 纳米团簇;  $Ca_{70}Mg_{30}$  合金; 快速凝固; 分子动力学模拟

(Edited by Chao WANG)